Available online at www.sciencedirect.com
SCIENCE DIRECT®
Bioorganic & Medicinal Chemistry Letters 14 (2004) 5367–5370
Bioorganic & Medicinal Chemistry Letters

Design, synthesis, and activity of 4-quinolone and pyridone compounds as nonthiol-containing farnesyltransferase inhibitors

Qun Li,* Akiyo Claiborne, Tongmei Li, Lisa Hasvold, Vincent S. Stoll, Steven Muchmore, Clarissa G. Jakob, Wendy Gu, Jerry Cohen, Charles Hutchins, David Frost, Saul H. Rosenberg and Hing L. Sham

Cancer Research, GPRD, Abbott Laboratories, Abbott Park, IL 60064-6101, USA

Received 29 June 2004; revised 6 August 2004; accepted 6 August 2004
Available online 3 September 2004

Abstract—As a part of our efforts to identify potent inhibitors of farnesyltransferase (FTase), modification of the structure of tipifarnib through structure-based design was undertaken by replacing the 2-quinolones with 4-quinolones and pyridones, and subsequent relocation of the D-ring to the *N*-methyl group on the imidazole ring. This study has yielded a novel series of potent and selective FTase inhibitors. The X-ray structure of tipifarnib (**1**) in complex with FTase was described.

Prenylation, a process of covalently attaching either a 15-carbon farnesyl moiety or a 20-carbon geranylgeranyl moiety to the conserved cysteine residues at the the C-terminus of certain proteins, plays a major role in a number of intracellular signaling pathways that control cell proliferation.[1] Among the important oncoproteins that require posttranslational prenylation for their activity is a family of Ras proteins.[2] Activating mutations of Ras are among the most common in human tumors.[3] The discovery that farnesylation is required for Ras transforming activity has led to an intense search for farnesyltransferase (FTase) inhibitors (FTIs) as anticancer agents.[4,5] Many FTIs have demonstrated excellent antitumor efficacy in preclinical human xenograft models and several compounds are now in Phase II/III clinical trials.[6,7] However, recent studies have shown that other farnesylated protein targets other than Ras, such as RhoB, may be more important for the antitumor effects of FTIs.[8]

Related to FTase is geranylgeranyltransferase I (GGTase I), which is responsible for the prenylation of 80–90% of prenylated proteins. Because FTIs have been shown to be sufficient for achieving growth inhibition in tumor cells and this effect is not enhanced with co-application of GGTase inhibitors,[9] selective FTIs

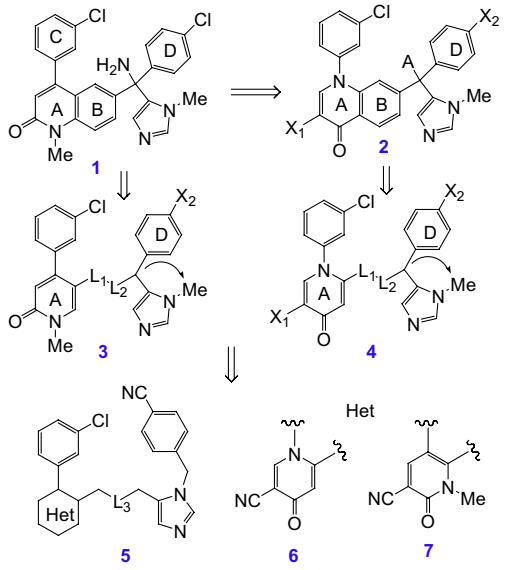

Figure 1. Modifications of tipifarnib (**1**) lead to novel inhibitors of FTase **2**–**7**.

Keywords: Farnesyltransferase inhibitors; Anticancer; Tipifarnib; Quinolone; Pyridone.
* Corresponding author. Tel.: +1 8479377125; fax: +1 8479361550; e-mail: qun.li@abbott.com

0960-894X/$ - see front matter © 2004 Elsevier Ltd. All rights reserved.
doi:10.1016/j.bmcl.2004.08.012

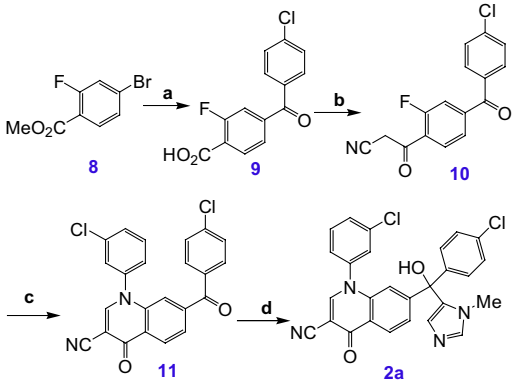

Scheme 1. Reagents and conditions: (a) (i) 4-Chlorophenylboronic acid, CO, $PdCl_2$ (dppf), K_2CO_3, anisole, 80 °C, overnight, 67%, (ii) LiOH, THF/H_2O, 70 °C, 1.5 h, 95%; (b) (i) $SOCl_2$, 80 °C, 15 min, (ii) *t*-BuO_2CCH_2CN, NaH, toluene, rt, (iii) TFA, CH_2Cl_2, 3 h; 61%; (c) (i) DMF–DMA, toluene, rt, 3 h, (ii) 3-chloroaniline, CH_2Cl_2, rt, (iii) K_2CO_3, pentanol, 110 °C, overnight, 34%; (d) (i) 1-methyl-2-TES-imidazole, *t*-BuLi, THF, −78 °C, 3 h, (ii) MeOH, 1 N HCl, rt, 0.5 h, 26%.

are sought in order to avoid potential undesirable toxicities.

Tipifarnib (R115777, **1**) is one of the most potent and selective nonthiol FTIs currently in Phase III clinical trials.[10] As a part of our efforts to identify novel and nonthiol FTIs, we report here our design and synthesis of a series of quinolone based FTIs (**2**–**7**) using the structure of tipifarnib as a template.

Synthesis of bicyclic 4-quinolone analog **2a** is illustrated in Scheme 1. The carbonylative cross-coupling of bromide **8** with 4-chlorophenylboronic acid using the condition of Ishiyama et al.[11], followed by saponification of the ester gave ketone **9** in 64% yield. Acid **9** was converted to cyanoacetone **10** in 61% yield via the reaction of its acid chloride with *t*-butyl cyanoacetate, and subsequent hydrolysis, and decarboxylation in TFA. Compound **10** was reacted with DMF–DMA to provide the *N*,*N*-dimethylenamine, which was further reacted with 3-chloroaniline then cyclized with K_2CO_3 in refluxing pentanol to afford cyano-4-quinolone **11** in 34% overall yield. The desired compound **2a** was prepared in 26% yield by the addition of 1-methyl-2-triethylsilyl-5-imidazolyl lithium[12] to the ketone (**11**) and subsequent removal of the triethylsilyl group with HCl in methanol.

Preparation of the required monocyclic 4-quinolone intermediates **16** and **17** is illustrated in Scheme 2. 4-Quinolone-3-carboxylic acid **14** was prepared from pyrone **12** in 59% overall yield by the method of Bassini et al.[13] Transformation of acid **14** to cyanide **15** was achieved in 91% yield by dehydration of the intermediate amide with $POCl_3$. Direct free radical promoted bromination of **15** gave the desired bromide **16** in low yield (⩽5%). The bromomethyl quinolone (**16**) was prepared alternatively from **15** in 26% yield by a three-step sequence involving oxidation to the aldehyde with SeO_2 in refluxing dioxane, reduction of the aldehyde to the alcohol with $NaBH(OAc)_3$, and reaction of the alcohol with PBr_3. Bromide **16** was then reacted with NaN_3 and the azido intermediate reduced with triphenylphosphine in refluxing THF/water to give amine **17** in 81% yield.

Reaction of aldehyde **18** with 1-methyl-2-triethylsilyl-5-imidazolyl lithium in the same way as described for **2a** provided alcohol **19** in 89% yield (Scheme 3). Coupling

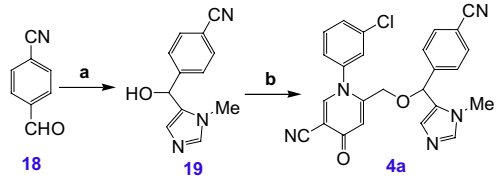

Scheme 3. Reagents and conditions: (a) (i) 1-methyl-2-TES-imidazole, *t*-BuLi, THF, −78 °C, 1 h, (ii) MeOH, 1 N HCl, rt, 0.5 h, 89%; (b) **16**, AgO, CH_2Cl_2, rt, 18 h, 44%.

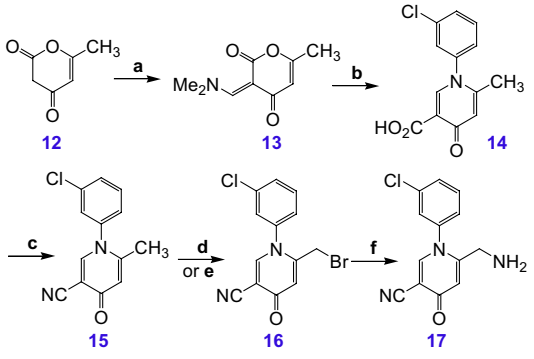

Scheme 2. Reagents and conditions: (a) DMF–DMA, toluene, rt, 4 h, 75%; (b) 3-chloroaniline, *t*-BuONa, EtOH, 90 °C, 18 h, 78%; (c) (i) CDI, DMF, 110 °C, 18 h, then NH_3, 4 °C, 18 h, 91%, (ii) $POCl_3$, NMP, rt, 3 h, 38%; (d) NBS, CCl_4, $PhCO_3H$, reflux, 18 h, 5%; (e) (i) SeO_2, dioxane, reflux, overnight, 77%, (ii) $NaBH(OAc)_3$, MeOH, rt, 4 h, 69%, (iii) PBr_3, LiBr, DMF, 0 °C, 4 h, 49%; (f) (i) NaN_3, acetone, reflux, 1 h, 91%, (ii) PPh_3, THF/H_2O, reflux, 1 h, 89%.

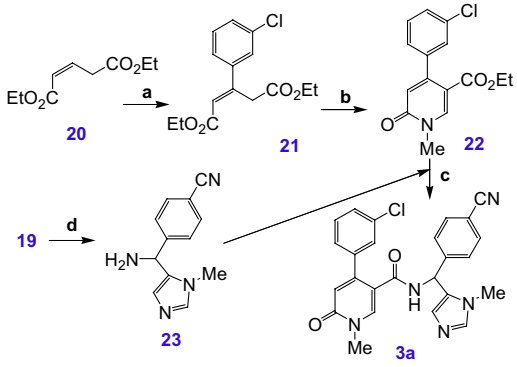

Scheme 4. Reagents and conditions: (a) 3-chloroiodobenzene, $Pd(OAc)_2$, NaOAc, DMF, 100 °C, 21 h, 20%; (b) (i) HCO_2Et, NaH, ether, rt, 2 h, 96%, (ii) $MeNH_2$, EtOH, reflux, 0.5 h, then, K_2CO_3, rt, 18 h, 41%; (c) (i) LiOH, THF/H_2O, 60 °C, 8 h, 77%, (ii) $(COCl)_2$, CH_2Cl_2, 0 °C to rt, 2 h, (iii) **23**, THF, rt, 18 h, 67%; (d) (i) $SOCl_2$, CH_2Cl_2, rt, 4 h, 100%, (ii) NH_4OH, THF, rt, 2 h, 77%.

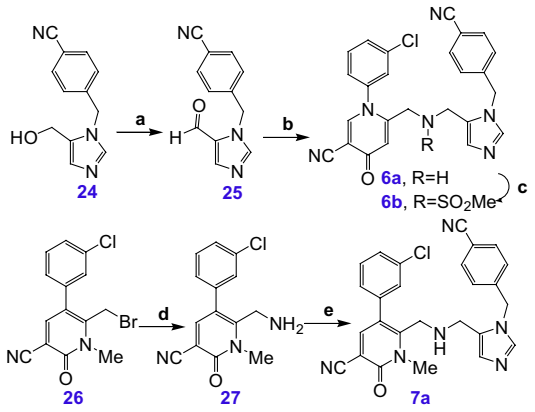

Scheme 5. (a) MnO_2, dioxane, 85 °C, overnight, 43%; (b) **17**, AcOH, MeOH rt, 1 h; then $NaBH_3CN$, rt, 1 h, 100%; (c) $MeSO_2Cl$, Et_3N, CH_2Cl_2, rt, 2 h, 18%; (d) (i) NaN_3, acetone, reflux, 1 h, 70%, (ii) PPh_3, THF/H_2O, reflux, 1 h, 83%; (e) **25**, AcOH, MeOH rt, 1 h; then $NaBH_3CN$, rt, 1 h, 71%.

of alcohol **19** with bromomethane **16** in the presence of silver oxide gave desired 4-pyridone analog **4a** in 44% yield.

Preparation of **3a** is shown in Scheme 4. The glutaconate (**20**) was converted to pyridone ester **22** according to the procedure of Kvita and Sauter in 8% overall yield.[14] In our hands, ester **22** could not be reduced to the alcohol without reducing the ring double bond. Thus it was hydrolyzed and converted to the acid chloride, which was coupled with amine **23** to furnish **3a** in 67% yield.

Synthesis of the analogs with the three-atom linkers (**6a** and **b**, and **7a**) is shown in Scheme 5. Thus 4-hydroxymethylimidazole **24**[15] was oxidized with MnO_2 to form aldehyde **25** (43% yield), which underwent reductive amination with **17** in the presence of sodium cyanoborohydride to give the desired product **6a** in 100% yield (Scheme 5). Reaction of **6a** with methanesulfonyl chloride produced sulfonamide **6b** in 18% yield. Reaction of bromomethyl 2-pyridone **26**[16] with sodium azide (70% yield) and subsequent reduction with triphenylphosphine gave amine **27** in 83% yield. Reductive alkylation of **27** with **25** furnished the desired product **7a** in 71% yield. In our hands, we were unable to couple alcohol **24** with either bromide **16** or **26** to form the ether-bridged compounds under a variety of reaction conditions.

The X-ray structure of tipifarnib in complex with FTase was obtained (Fig. 2a).[17,18] The result is similar to a recent work by Reid and Beese.[19] The imidazole serves as a replacement of the thiol of the CaaX tetrapeptide substrate by coordinating with the catalytic zinc that is critical to the farnesylation process. The 2-quinolone ring extends over the loop consisting of Asp359, Phe360, and Tyr361 and is lined from above the plane by residues Leu96 and Tyr93 via van der Waals interactions. The two chlorophenyl rings (rings C and D) occupy the two adjacent hydrophobic pockets and stack together forming a strong π/π interaction. The primary amine is not interacting directly with the protein, but is solvent exposed.

Table 1. Activity of quinolone based farnesyltransferase inhibitors

Compd	IC_{50} (nM)		EC_{50} (nM)
	FT[b]	GGT[c]	Ras processing[a]
2a	12	16,000	51%[d]
3a	685	nt[e]	nt[e]
4a	12	>10,000	4%[d]
6a	7.9	>10,000	0%[d]
6b	160	nt[e]	nt[e]
7a	17	>10,000	21%[d]
Tipifarnib (**1**)[f]	0.65	1100	1.6
Lonafarnib[f,21]	8.3	>10,000	100

[a] In H-Ras NIH-3T3 cells.
[b] Bovine farnesyltransferase.
[c] Bovine geranylgeranyltransferase.
[d] Inhibition at 100 nM.
[e] Not tested.
[f] Data from racemic mixtures.

Having a carbonyl group rather than a methyl group facing solvent front, the X-ray structure suggests the 4-quinolone (**2**) should be a good mimic of **1**. A carbonyl group in **2** now faces the solvent front versus a methyl group in **1** and the cyano group in 4-quinolone now replaces the 2-carbonyl group in **1**. Indeed, **2a** was found to be a potent and selective inhibitor of FTase, with IC_{50} values[20] of 12 nM and 16 μM against FTase and GGTase, respectively (Table 1). The inhibition of Ras processing in H-Ras transformed cells[20] was determined as a measure of intracellular potency. Compound **2a** shows an EC_{50} of about 100 nM.

Structure analysis revealed that it might be possible to maintain the desired conformation by deleting the B-ring in **1** and **2**, provided that an appropriate and accessible linker is used. Thus pyridones **3a** and **4b** were designed and synthesized, wherein the pyridone and imidazole moieties are connected via amide bond and ether linkages, respectively. The amide **3a** is significantly less potent than **1** with an IC_{50} of 685 nM against FTase. Unlike the amide, ether **4a** displays very good FTase activity (IC_{50} 12 nM) that is identical to 4-quinolone **2** and only about 17-fold higher than **1**. EC_{50} of Ras processing for one of the compounds tested (**4a**) was determined to be over 100 nM.

Examination of the structures of **3** and **4** revealed that the D-ring (Fig. 1) could be attached to the adjacent *N*-methyl group on the imidazole ring without significantly affecting its binding to the hydrophobic pocket of FTase. This modification not only simplifies the synthesis, but also makes the compounds achiral. 4-Pyridone analog **6a** is the most potent FTase inhibitor synthesized with an IC_{50} of 8 nM, which is slightly more active than its parent **4a**. 2-Pyridone **7a** is about 2-fold less potent than the 4-pyridone (**6a**). Attaching a methanesulfonyl group on the linker nitrogen in **6a** resulted in a 20-fold drop in FTase activity. Compound **6a** shows poor activity in Ras processing assay and has an EC_{50} over 100 nM. None of the compounds in this series are active against GGTase with IC_{50} values over 10 μM.

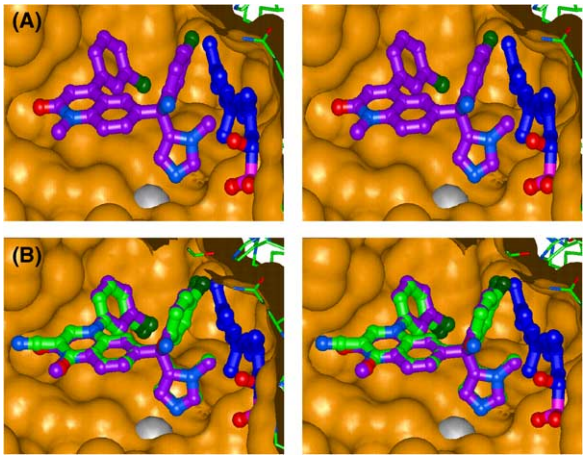

Figure 2. Stereo views of (**A**) tipifarnib and (**B**) an overlay of a model of compound **2a** (in green) over the X-ray crystal structure of tipifarnib (**1**) (in purple) in complex with FTase in the active site. Zn^{+2} is shown in grey and hydroxy farnesylpyrophosphate in blue.

Stereo view of an overlay of a model of **2a**, which was modeled based on the crystal structure of a close chemical analog[22] and the X-ray crystal structure of tipifarnib (**1**) is shown in Figure 2b. The model of **2a** superimposes very well with tipifarnib. The important cyano group of **2a** binds to the main chain loop consisting of residues Asp359, Phe360 and Tyr361 through a combination of electrostatic and van der Waals interaction.

In summary, we have used the structure of tipifarnib to design a series of novel inhibitors of FTase. The compounds demonstrate potent activity against FTase with IC_{50} values in the nanomolar range. The current series of compounds are highly selective and their IC_{50} values against GGTase are in the double-digit micromolar range. The successful discovery of 4-quinolone **2** as a potent FTase inhibitor has opened a door for future opportunities to extend further into other 4-quinolones and bicyclic 2-pyridones.[23] However, further structural modifications are needed in order to improve the cellular activity of the current series. These efforts have led to the discovery of more potent FTase inhibitors, the detailed of which will be presented elsewhere[16,22,24] and in the subsequent paper in the current journal.

Acknowledgements

X-ray crystallographic data were collected at beamline 17-ID in the facilities of the Industrial Macromolecular Crystallography Association Collaborative Access Team (IMCA-CAT) at the Advanced Photon Source. These facilities are supported by the companies of the Industrial Macromolecular Crystallography Association.

References and notes

1. Hurwitz, H. I.; Casey, P. J. *Curr. Top. Membranes* **2002**, *52*, 531–550.
2. Downward, J. *Nat. Rev. Cancer* **2003**, *3*, 11–22.
3. Bos, J. L. *Cancer Res.* **1998**, *49*, 4682–4689.
4. Ayral-Kaloustian, S.; Salaski, E. J. *Curr. Med. Chem.* **2002**, *9*, 1003–1032.
5. Singh, S. B.; Lingham, R. B. *Curr. Opin. Drug Dis. Dev.* **2002**, *5*, 225–244.
6. Dancey, J. E. *Curr. Pharm. Des.* **2002**, *8*, 2259–2267.
7. Purcell, W. T.; Donehower, R. C. *Curr. Oncol. Rep.* **2002**, *4*, 29–36.
8. Hluska, P.; Dy, G. K.; Adjei, A. A. *Eur. J. Cancer* **2002**, *38*, 1685–1700.
9. Sebti, S. M.; Hamilton, A. D. *Exp. Opin. Invest. Drugs* **2000**, *9*, 2767–2782.
10. Norman, P. *Curr. Opin. Invest. Drugs* **2002**, *3*, 313–319.
11. Ishiyama, T.; Kizaki, H.; Hayashi, T.; Suzuki, A.; Miyaura, N. *J. Org. Chem.* **1998**, *63*, 4726–4731.
12. Molina, P.; Fresneda, P. M.; Garcia-Zafra, S. *Tetrahedron Lett.* **1996**, *37*, 9353–9356.
13. Bassini, C.; Bismara, C.; Carlesso, R.; Feriani, A.; Gaviraghi, G.; Marchioro, C.; Perboni, A.; Shaw, R. E.; Tamburini, B.; Tarzia, G.; Xerri, L. *Farmaco* **1993**, *48*, 159–189.
14. Kvita, V.; Sauter, H. *Angew. Chem., Int. Ed. Engl.* **1987**, *26*, 790–791.
15. Williams, T. M.; Bergman, J. M.; Brashear, K.; Breslin, M. J.; Dinsmore, C. J.; Hutchinson, J. H.; MacTough, S. C.; Stump, C. A.; Wei, D. D.; Zartman, C. B.; Bogusky, M. J.; Culberson, J. C.; Buser-Doepner, C.; Davide, J.; Greenberg, I. B.; Hamilton, K. A.; Koblan, K. S.; Kohl, N. E.; Liu, D.; Lobell, R. B.; Mosser, S. D.; O'Neill, T. J.; Rands, E.; Schaber, M. D.; Wilson, F.; Senderak, E.; Motzel, S. L.; Gibbs, J. B.; Graham, S. L.; Heimbrook, D. C.; Hartman, G. D.; Oliff, A. I.; Huff, J. R. *J. Med. Chem.* **1999**, *42*, 3779–3784.
16. Hasvold, L. A.; Wang, W.; Gwaltney, S. L.; Rockway, T. W., II; Nelson, L. T. J.; Mantei, R.; Fakhoury, S.; Sullivan, G.; Li, Q.; Lin, N.-H.; Wang, L.; Zhang, H.; Cohen, J.; Gu, W.-Z.; Marsh, K.; Bauch, J.; Rosenberg, S.; Sham, H. *Bioorg. Med. Chem. Lett.* **2003**, *13*, 4001–4005.
17. Protein of the Rat Ftase was purified and crystallized in the presence of HFP and Ac-CVIM peptide according to the methods outlined in Strickland et al.[18] Crystals of Ftase were soaked in a solution containing 0.1 M KCl, 0.1 M sodium acetate pH 4.7 saturated with tipifarnib. The structure was refined to 3.5 Å resolution with an $R = 22.31\%$ and $R_{free} = 29.19\%$. Crystallographic data for structure of tipifarnib in complex with FTase in this paper have been deposited with PDB (ID: 1X81).
18. Strickland, C.; Windsor, W. T.; Syto, R.; Wang, L.; Bond, Ri.; Wu, Z.; Schwartz, J.; Le, H. V.; Beese, L. S.; Weber, P. C. *Biochemistry* **1998**, *37*, 16601–16611.
19. Reid, T. S.; Beese, L. S. *Biochemistry* **2004**, *43*, 6877–6884.
20. Assay methods described in: Vogt, A.; Qian, Y.; Blaskovich, M. A.; Fossum, R. D.; Hamilton, A. D.; Sebti, S. M. *J. Biol. Chem.* **1995**, *270*, 660–664.
21. Wang, L.; Johnson, W. W. *Chemotherapy* **2003**, *49*, 303–308.
22. Wang, L.; Wang, G. T.; Wang, X.; Tong, Y.; Sullivan, G.; Park, D.; Leonard, N.; Li, Q.; Cohen, J.; Gu, W.-Z.; Zhang, H.; Bauch, J.; Jacob, C. G.; Hutchins, C. W.; Stoll, S. V.; Marsh, K.; Rosenberg, S. H.; Sham, H.; Lin, N.-H. *J. Med. Chem.* **2004**, *47*, 612–626.
23. Li, Q.; Mitscher, L. A.; Shen, L. L. *Med. Res. Rev.* **2000**, *20*, 231–293.
24. Tong, Y.; Lin, N.-H.; Wang, L.; Hasvold, L.; Wang, W.; Leonard, N.; Li, T.; Li, Q.; Cohen, J.; Gu, W.-Z.; Zhang, H.; Stoll, V.; Bauch, J.; Marsh, K.; Rosenberg, S. H.; Sham, H. L. *Bioorg. Med. Chem. Lett.* **2003**, *13*, 1571–1574.